



RECONSTRUCTION CREASE FOR FINGERPRINT IMAGES USING MINUTIA DENSITY DISTRIBUTION: AN EMPIRICAL STUDY

Firas S. Abdulameer^{1*}

Kuba Hasanien Kariem²

¹Department of physics, College of Science, Mustansiriyah University, Baghdad, Iraq.

²Biomedical Informatics College, University of Information Technology and Communication, Baghdad, Iraq

Email: fitasalaraji@uomustansiriyah.edu.iq, hasanien.k.a@uoitc.edu.iq

Article history:	Abstract:
Received: 26 th June 2022 Accepted: 26 th July 2022 Published: 6 th September 2022	Fingerprint recognition is one of the secure techniques for automatic personal identification, and it is one of the safe techniques for automatic personal identification. . It is receiving more and more attention and is frequently used in civil applications like access control and financial security. One of the critical elements in image processing applications that refer to human traits for user verification is the fingerprint. In real terms, wrinkles will split ridgelines and create a string of false minutiae, fatally destroying the structure and texture of a fingerprint. Wrinkles will thereby decrease the accuracy of the fingerprint identification algorithm, especially in the leading technique based on minutiae-matching. In this article, we investigate two elements of the treatment of wrinkles and ridge reconstruction using fingerprint photos. To start, we calculate the distance between pseudo minutiae pairing. Then, we reconstruct ridges based on midpoint criteria of a line segment with endpoints. The outcomes are presented in the paper.

Keywords: Fingerprint recognition; Creases recognition; Wrinkles repair; Minutia density.

INTRODUCTION

As the significance of automatic person identification applications increases, fingerprint-based identification is getting much attention. The fingerprint is the most trustworthy proof for labeling among the biometric data that is now available, including the face, speech, iris, and gesture. Feature extraction, data collecting, and matching are the three main stages of a general fingerprint recognition system [1]. Due to their resistance to various sources of fingerprint degeneration, the end and bifurcation of ridges serve as the fingerprint's primary representation for the stage of fingerprint matching. For instance, minutiae are the foundation upon which the ANSI-NIST standard fingerprint description is created [2]. Miniature detection and matching heavily depend on ridge orientation estimation and image segmentation, even though ridge orientation is invariably used for checking, describing, and sensing minutiae. Accurate image segmentation helps avoid detecting artificial minutiae in low-quality image areas [2, 3].

Minuet-primary extraction removes little details from a fingerprint following preprocessing techniques like binarization, enhancement, thinning, etc. The matching phase, as the name suggests, involves comparing two fingerprints to ascertain if they are from the same finger or not. Accurate minutiae extraction with more tiny omissions or erroneous extractions is significant for performance improvement for a minutiae-based recognition system.

Numerous strategies, including the gradient scheme, Slit, projection-based techniques, the Gray-level consistency/variance technique, and calculations in the frequency region, have recently been used to estimate the orientation field (OF) of fingerprint patterns [4, 5]. Because of its superior performance and resolution compared to other methods, gradient squared averaging is typically used to determine the orientation field of a picture block [6–9]. The estimation of an orientation map (OM) may not be accurate because gradient extraction is susceptible to noise and flaws [10]. In contrast, an orientation smoothing stage can solve this issue and improve the ridge structure representation for fingerprint classification. Numerous strategies, including the gradient scheme, Slit, projection-based techniques, the Gray-level consistency/variance technique, and calculations in the frequency region, have recently been used to estimate the orientation field (OF) of fingerprint patterns [4, 5]. Because of its superior performance and resolution compared to other methods, gradient squared averaging is typically used to determine the orientation field of a picture block [6–9]. The estimation of an orientation map (OM) may not be accurate because gradient extraction is susceptible to noise and flaws [10]. In contrast, an orientation smoothing stage can solve this issue and improve the ridge structure representation for fingerprint classification. The quality of fingerprint images hardly influences the accuracy of the recognition algorithm. Some poor fingerprint images will lead to extracting minutiae mistakenly and error matching. One of the unfortunate images is occupied by creases distinguished by collinear terminations on ridges

[4]. Fortunately, it can repair creases. Jian et al. [3] and Zhou J et al. [10, 11] indicate that wrinkles often appear in fingerprint recognition for older adults. However, influenced by the precision of the sensor, the skin dryness, wounds, dirt, oil stain, etc., the captured fingerprint images are quickly clouded by creases, even if Youngers assesses them. Case detection and repair are required to improve recognition accuracy while processing some poor-quality fingerprint images. The wrinkles will split up the normal ridgelines, producing several pseudo minutiae in these areas. Because of this, we propose an approach to detect wrinkles based on the Minutia Density (MD) distribution. First, calculate the distance between pseudo minutiae pairing. Second, we reconstruct ridges based on midpoint criteria of a line segment with endpoints. The results show an apparent increase in recognition accuracy after crease repair.

The rest of the document is organized as follows: Section 2 describes the fingerprint recognition algorithm. A brief description of the linked works is provided in Section 3. which proposes an algorithm for ridge reconstruction and crease detection based on the methodology in Section 4. The findings and recommendations are presented in Sections 5 and 6, respectively.

RELATED WORK

Fingerprints are the appearances or imprints left by a person's fingers on a surface. They are used to identify people based on the distinctive whorls and ridges on their fingertips. The challenging field of fingerprint crease detection has attracted very few researchers. Finding creases is quite difficult due to the roughness of fingerprints. It is challenging to distinguish the wrinkles from other features on the fingerprint due to their crowded background. It can be difficult to identify the crease(s) in a fingerprint because valleys and wrinkles frequently resemble one another. Fingerprint valleys are hollow channels that lie in between ridges. The creases are also known to cut across the ridges and valleys at an angle that is typically wide enough to distinguish them from the valleys. Visual observations suggest that most wrinkles are at an angle of more than 20 degrees to the ridge and valley structure. Therefore, designing a crease detection algorithm requires many assumptions to differentiate a crease from a valley distinctively. Some of the hypotheses presented by other researchers include observing the essential characteristics of a crease such as a length, width, pixel intensity, etc [12, 13, 30, 31, 32 and 33]. For instance, Gottschlich et al. [14] provided a novel method for OF estimate based on traced ridge and valley lines. This method is resistant to perturbations caused by scars, wetness, pollution, or finger dryness, for example. The line-sensor method is compared to a gradient-based approach and a multiscale directional operator in terms of performance. Experiments with simulated scar noise drawn on top of good quality fingerprint pictures from the FVC2000 and FVC2002 databases are used to test its resilience. Lastly, the effectiveness of the line-sensor-based method is demonstrated on 60 generally poor quality fingerprint images from the FVC2004 database. Wu et al. [10] studied a novel pattern in the fingerprint called crease, a kind of stripes irregularly crossing the standard fingerprint patterns (valleys and ridges). Wrinkles will cause spurious minutiae by using conventional feature detection algorithms, decreasing the recognition rate of fingerprint identification. The author creates an optimum detector and uses a multi-channel filtering framework to identify wrinkles in various orientations by expressing the crease with a parameterized rectangle. PCA is applied in each channel to derive rectangle parameters from raw detected data. Jian et al. [3] proposed an innovative method for crease detection and correction based on minutia density distribution. From Minutia Density distribution, creases are separated from others and then classified into SODCAs and LODCAs. The orientation field distribution differs significantly, and the pseudo minutiae pairings are hard to unite in two kinds of crease areas. In SODCAs, we adopt Least Deviation for minutiae pairing and stepwise approximate for reconnections. In LODCAs, the Normal calibration technique and the triangular constraint method are more suitable. The results confirm that the algorithm can repair and detect creases efficiently, and the recognition accuracy enhances significantly with wee supplementary calculations. Chauhan et al. [15] searched the use of crease features for fingerprint classification. Experiments are conducted on the Hong Kong PolyU high-resolution fingerprint database DBII, which is open to the public. The experimental results are very supportive and show that creases have huge potential to enhance the performance of fingerprint classification. Chen et al. [16] proposed a new algorithm to utilize minutiae for fingerprint recognition. The orientation field of a fingerprint is reconstructed from minutiae and employed in the matching step to improve the system's performance. First, we use interpolation in the sparse area to show "virtual" minutiae, and then we use an orientation model to rebuild the orientation field from all "virtual" and "real" minutiae. The reconstructed orientation field matching and traditional minutiae-based matching are combined using a decision fusion approach. The proposed strategy can generate more accurate results than existing methods since the orientation field is an essential global property of fingerprints. Bian et al. [4] devoted to reviewing and categorizing many Fingerprint orientation field (FOF) estimation techniques introduced in the specialized literature, focusing on the most modern work in this area. Existing FOF estimation techniques can be grouped into three categories: mathematical models-based methods, gradient-based methods, and learning-based techniques. Explaining and identifying the advantages and limitations of these FOF estimation methods is of significant significance for fingerprint identification because only a complete understanding of the nature of these methods can shed light on the essential issues for FOF estimation. The authors present a comprehensive discussion and analysis of these methods concerning their advantages and limitations. They have also handled tests utilizing publically available competition datasets to efficiently compare the achievement of the most relevant algorithms and techniques. A new fingerprint orientation field reconstruction approach was presented by Weixin et al. [17]. The main goal of the technique is to reorient the ridge using orthogonal polynomials in two discrete variables and the best quadratic approximation. Using the best quadratic approximation provided by orthogonal polynomials in two discrete variables in the sine domain, reconstruct the ridge

orientation field after first estimating the local region orientation using linear projection analysis (LPA) based on the vector set of point gradients. The suggested method can more accurately and robustly estimate the FOF of low-quality fingerprint pictures with significant noise areas. Gupta et al. [27] a new approach that takes into account the details has been proposed. For the fingerprint reconstruction, consider density and the orientation field direction. For the analytical outcomes and to test the suggested approaches for fingerprint reconstruction, the public domain datasets Fingerprint Identification Competition 2002 (FVC2002) and Fingerprint Verification Competition 2004 (FVC2004) have been employed. Brancati et al. [28] offered a new method for reconnecting broken ridges in fingerprint photographs in this paper. The technique determines ridge direction by using a discrete directional mask and the gray-level standard deviation. The obtained direction map is smoothed by counting the occurrences of the rules in a suitably broad window. After that, the fingerprint pictures are binarized and thinned. A morphological transformation guides the process of creating linking routes to connect fractured ridges.

One immediate result discovered when researching the structural problems caused by wrinkles is that wrinkles produce a large number of pseudo minutiae. The minutiae number is much higher than the minutiae number in normal ranges of the same size. As a result, we offer a unique method for detecting and reconstructing wrinkles in fingerprint images based on the Minutia Density distribution (MDD). The results reveal that the approach may effectively witness Minutia pairing and rebuild the next point of ridges.

RECONSTRUCTION CREASE FOR FINGERPRINT IMAGES

There are numerous approaches that may be broadly categorized as gradient [18–20], orientation field modeling methods [4, 21, 22], neural network approach [23, 24], and ridge projection method [25, 26]. Many individuals have worked on the topic of fingerprint ridge orientation.

DETECTION OF WRINKLE

A small amount of false or missing minutiae will cause a dramatic decline in accuracy for a minutiae-based algorithm. The creases will sever distinct ridges, and a sequence of pseudo-minutiae will be introduced. This so-called pseudo-minutiae typically takes the form of endpoints; because the wrinkle cuts ridges, one or more endpoints may be born on either side of the crease. The fact that the crease areas frequently lack contrast only complicates matters further. The background, valleys, and ridges are difficult to separate. Some initially parallel ridges that cross each other in crease areas might create pseudo-bifurcates or even pseudo-singular points, as seen in Fig. 1. (c). In conclusion, creases will alter the local structure, create fictitious details, and change the overall design, including orientation and frequency field distribution. The pseudo-minutiae must be connected correctly, with fewer errors between distinct creases or more common ridges. Reconnections between these details will lessen the damage to the fingerprint's original structure. According to Zhou J et al., the wrinkles maintain their stability for an extended period, making them useful as independent features and different characteristics for fingerprint matching [11]. Finding creases and precisely identifying their classification must come first. The minutia density is the number of minutiae in a particular area after minutia extraction (MD). The MD values are tiny and the minutia distribution is dispersed in public spaces. The pseudo minutiae result in a much bigger MD in wrinkle zones. We can now identify big MD areas as crease prospects. According to the distribution of the orientation field around the target point, we sketch a fixed size $G * K$ orthogonal box, as illustrated in Fig. 2. A straight orientation field defines the edge G . The orientation field is vertical to the edge K .



Figure 1. (a) A distinct image (b) Image filtering (c) Extracted minutiae from the fingerprint

The G, K values are related to the wrinkle's length and breadth. If the numbers are too small or too great, the differences in the crease and common sections will become blurry. The wrinkle candidate region is indicated if the MD value at position (x, y) is behind TH_{md} .

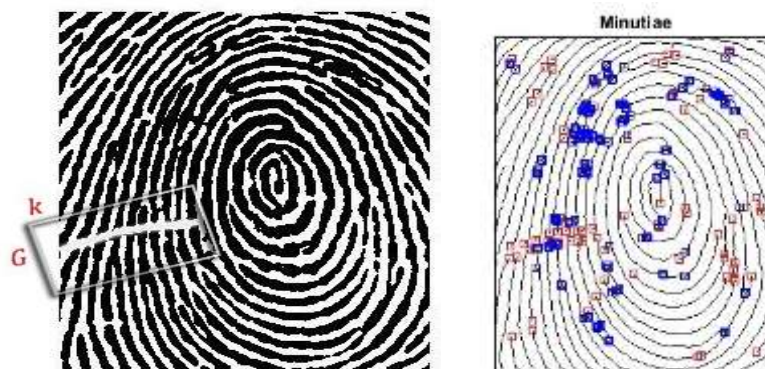


Figure 2. The MD calculation diagram

$$TH_{md} = num / (G \cdot K) \tag{1}$$

Zhou et al. [11] and Jian et al. [3] set some limitations for the crease model, which can improve screening out accurate wrinkles from candidates, as shown below:

$$w > TH1, \quad l > TH2, \quad \text{and} \quad l/w > TH3 \tag{2}$$

$$avg\{L(Cx, Cy, l, \phi)\} > TH4 \tag{3}$$

$$\phi > TH5 \tag{4}$$

Where $L(Cx, Cy, l, \phi)$ represents the wrinkle curve, (Cx, Cy) , w , l and ϕ are the middle points coordinate, width, length, and wrinkle orientation L , individually. Each $avg\{L(Cx, Cy, l, \phi)\}$ indicates average grayscale of the wrinkle L . ϕ is the orientation variance among the wrinkle curve and regular ridges. TH1, TH2, TH3, TH4, and TH5 are all tentative values. The wrinkle detection schematic description is presented in Fig. 3.



Figure 3. (a) Target fingerprint image, (b) Large MD areas in the image shown as blue strips

Wrinkles' Reconstruction and Repair

We deal with the ridges and creases of a fingerprint in this section. The objectives are to calculate the separation between two pairs of fictitious minutiae and reconstruct ridges. We present our strategy in two primary steps:

Step 1: Pseudo of Minutiae Pairing

Pseudo-minutiae are shown in almost identical amounts in Fig. 5. This zone has eight pseudo-minutiae that are designated separately as $A_1 - A_4$ and $a_1 - a_4$,

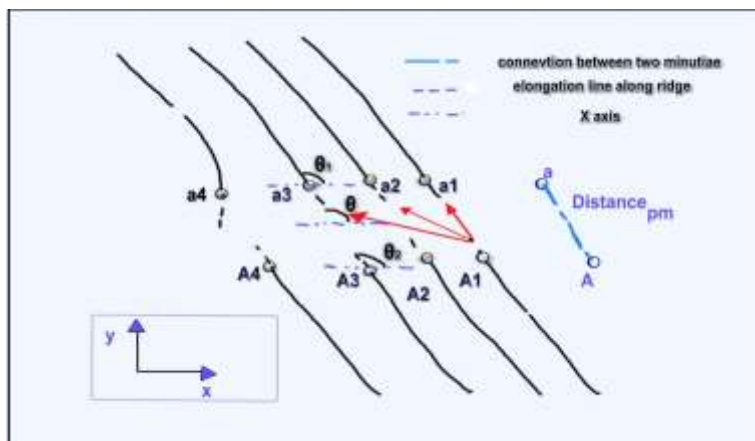


Figure 4. Diagram of eight ridge minutiae

The two orientation values of the minutiae pairing, θ_1 and θ_2 , the distance_{pm} between them, and the angle between the x-axis and two-point connection are the four key parameters for each pairing sample. Since the pseudo minutiae, as previously indicated, are almost equivalent, we assume that the angle is constant, meaning that the orientation values, θ_1 and θ_2 , are constant. Now, we use the following equation to determine the separation between two paired ends of pseudo minutiae.

$$\text{Distance}_{pm} = \sum_{k=1}^M \sum_{z=1}^N \sqrt{(A_k - a_z)^2} \tag{5}$$

Where Distance_{pm} the distance between two pairing ends of pseudo minutiae is, $A = \{A_1, A_2, A_3, \dots, A_k\}$ $a = \{a_1, a_2, a_3, \dots, a_z\}$ is the set of end ridge and the set of an opposite ridge, individually. According to Equations (5) then we get stacks which are defined as follows

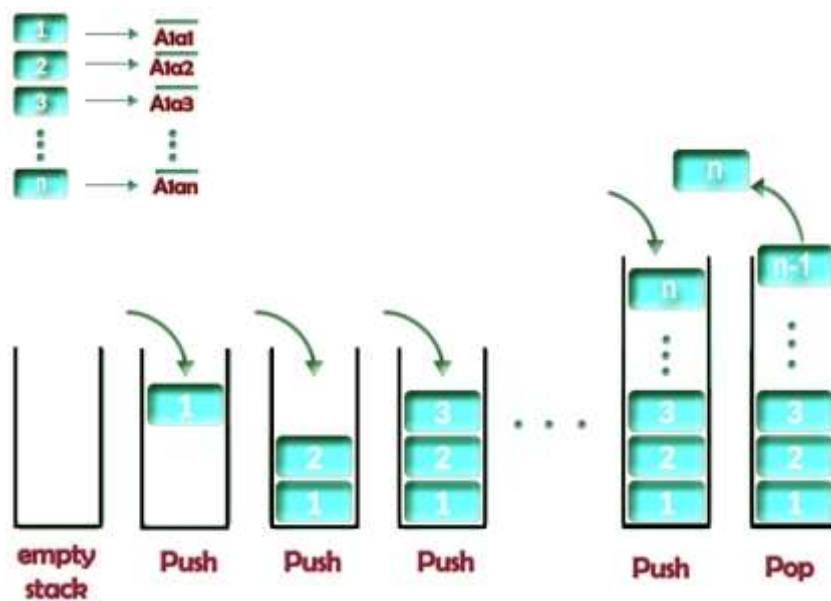


Figure 5. Diagram of Stacks

Subsequently, we select the most negligible value that satisfies Eq. (5) constraints, then, we can obtain $A_1 - a_1, A_2 - a_2, A_3 - a_3$, and $A_4 - a_4$ minutiae pairs. Between two ridgelines, the distance varies from 5 to 23 pixels [11-14]. The dotted line in Fig.6 indicates the ridgeline's extension line with the direction, whereas the solid line denotes the ridgeline's standard line at point A_2 . Points A_3 and A_2 are on opposite sides of the regular line, however at point Q , the normal line inserts a ridgeline. On the same ridgeline as Point Q and A_3 . Now, if the Euclidean distance between points C and A is less than 23 pixels, we can deduce that they are also on the same side of the standard line. Points a_2, a_1 , and a_3 are the remaining candidates. They're all on the opposite side of A_2 . The closest point is chosen as A 's partnering point based on distance estimates. Similarly, $A_1 - a_1$ and $A_3 - a_3$ pairs can be found.

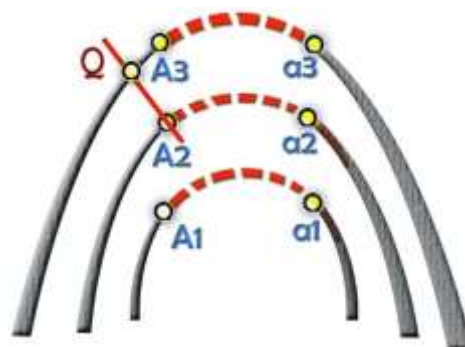


Figure 6: Distribution of fingerprints and minutiae

Step 2: Reconstruction of Minutiae pair

After pairing, now we will choose the next points based on midpoint criteria of a line segment with endpoints. Our steps are explained below:

1. We choose a point (i.e., next point) in the middle of the curve between minutiae pairing, as shown in Fig. 9, to get x and y values of the next point based on the following formula.

$$M\left(\frac{x_1 + x_2}{2}, \frac{y_1 + y_2}{2}\right) \quad (6)$$

For instance, we assume that the $A_1(x_1, y_1) = (-3, 2)$ and $a_1(x_2, y_2) = (5, -2)$.

$$M = \left(\frac{-3 + 5}{2}, \frac{2 + (-2)}{2}\right)$$

$$M = \left(\frac{2}{2}, \frac{0}{2}\right) = M(1, 0)$$

Now, the midpoint coordinates between A_1 and a_1 are $(1, 0)$ as shown in Fig. 9.

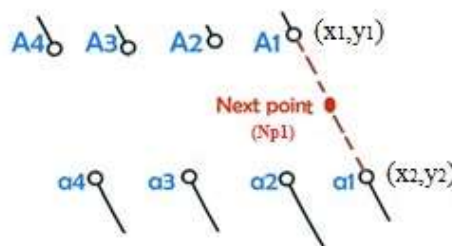


Figure 9. Determine the next minutiae point

2. We find the next point N_{p2} between the old points (calculated in the previous step(N_{p1})) and A_1 based on Equ.6 as shown in Fig.10.

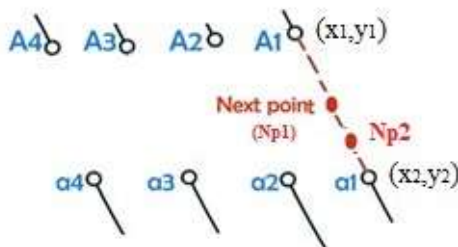


Figure 10. Determine the N_{p2} point

3. We find the next point N_{p3} between the old points (calculated in the previous step(N_{p1})) and a_1 based on Equ.6 as shown in Fig. 11.

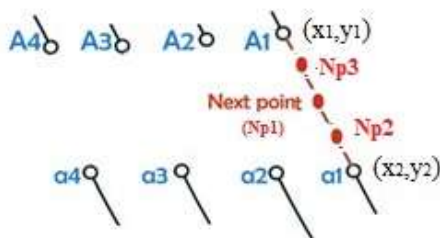


Figure 11. Determine the N_{p3} point

The spurious minutiae have all been eliminated in Fig. 9. The orientation field and frequency field are then recalculated. In the crease-unrepaired image, the orientation field is twisted, whereas, in the restored image, it is more consistent with texture. As a result of the crease-repair, the algorithm's accuracy increased significantly.

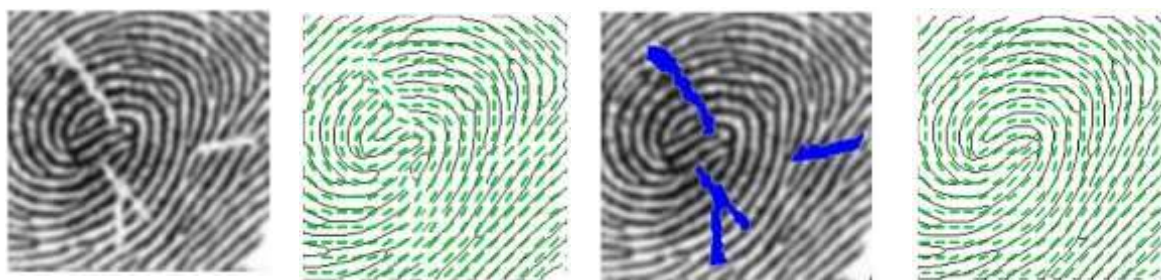


Figure 12. The detection and correction of creases is shown schematically in this diagram. Endpoints are coloured blue, bifurcations are coloured green, and core points are coloured red. (a) Use a grayscale fingerprint image as your input. (b) Blue stripes indicate where the folds are. (c) The unrepaired image's orientation field (d) The image's restored orientation field.

EXPERIMENTAL OUTCOMES

The experiments in this section compare the performance of our algorithm to methods elaborated in the Zhou J. method [11], conventional method, and Jian W. method [3]. Experiments with the three methods listed above. The database contains 100 individual fingers, 20 of which are from the same finger. Algorithms are evaluated using the False Reject Rate (FRR), False Accept Rate (FAR), ZeroFAR, ZeroFRR, ERR, FAR1000, and time-cost. The results show that the method may improve the reconstruction of the wrinkles of fingerprint by determining the next point of minutiae pairing. The results (Fig. 13) demonstrate that our strategies significantly improve performance. In the low FAR area, our technique surpasses Zhou J, but in the high FAR area, it is defeated. In actual applications, FAR must be kept to a minimum. In terms of ERR, ours is (5.372%) higher than Jian's (5.482%), Zhou's (5.722%), and the usual technique (5.852%), as indicated in Table I. Our method is less computational than Zhou J's and Ian W. since we don't use any additional convolution operations. As a result, when compared in an experiment, time-cost (219.014ms) outperforms Jian's (223.013ms) and Zhou J's (347.423ms). Because of its superior performance in low FAR areas and minimal computation, our method outperforms others in practice.

Table I. Four distinct approaches performance

Performance	Conventional method[3]	Zhou J method[11]	Jian method[3]	W.	Our method
Time-cost	206.9335ms	347.423ms	223.013ms		219.014ms
ZeroFAR	0.3854	0.2276	0.2192		0.2085
ZeroFRR	0.9406	0.9126	0.9141		0.9120
ERR	0.05852	0.05722	0.05482		0.05372
FAR1000	0.1616	0.1096	0.1064		0.1053

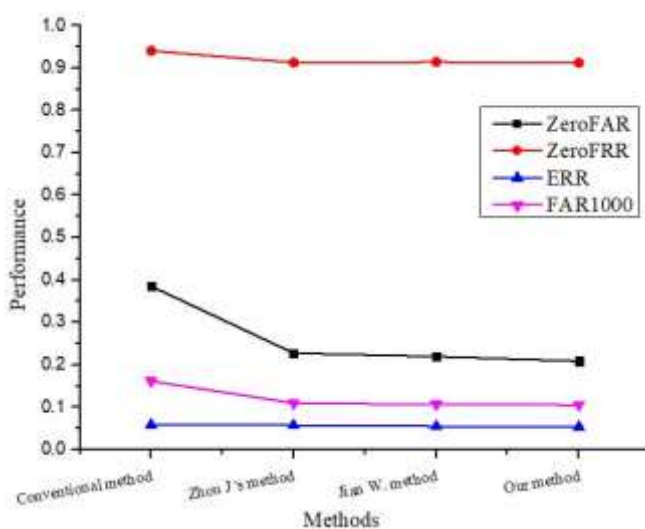


Figure 13. Performance of Four approaches

CONCLUSION

In this study, we provide a novel technique for reconstructing the fingerprint. This research examined fingerprint image wrinkle detection. The two-step procedure serves as the foundation for the reconstruction of fingerprints given in this work, enhancing two areas of wrinkle reconstruction performance in recognizing fingerprints. The distance between pairs of pseudominutiae was first estimated. Second, by figuring out the next point of minutiae pairing, we rebuild the ridges based on the midway criteria of a line segment with ends. The findings demonstrate that artificial minutiae can be used to recreate ridges to improve fingerprint identification. For upcoming work, we'll concentrate on combining different methodologies to achieve a improved performance of fingerprint identification with creases.

REFERENCES

- [1] M. NarayanMohanty and R. Sikka, "oReview on fingerprint-based identification system," *Materials Today: Proceedings*, 2021.
- [2] L. N. Darlow and B. Rosman, "Fingerprint minutiae extraction using deep learning," in *2017 IEEE International Joint Conference on Biometrics (IJCB)*, 2017, pp. 22-30: IEEE.
- [3] W. Jian, Y. Zhou, H. Liu, and N. Zhu, "Crease Detection and Repair Based on Minutia Density Distribution," in *2019 IEEE 11th International Conference on Communication Software and Networks (ICCSN)*, 2019, pp. 446-451: IEEE.
- [4] W. Bian, D. Xu, Q. Li, Y. Cheng, B. Jie, and X. Ding, "A survey of the methods on fingerprint orientation field estimation," *IEEE Access*, vol. 7, pp. 32644-32663, 2019.
- [5] R. Gupta, M. Khari, D. Gupta, and R. G. Crespo, "Fingerprint image enhancement and reconstruction using the orientation and phase reconstruction," *Information Sciences*, vol. 530, pp. 201-218, 2020.
- [6] A. A. ABBOOD, G. SULONG, A. M. TAHA, and S. U. PETERS, "A new technique for estimating and enhancing orientation field of fingerprint image," *Journal of Theoretical and Applied Information Technology*, vol. 96, no. 7, 2018.
- [7] C. Yuan and X. Sun, "Fingerprint liveness detection using histogram of oriented gradient based texture feature," *Journal of Internet Technology*, vol. 19, no. 5, pp. 1499-1507, 2018.
- [8] E. P. Wibowo, S. A. Harseno, and R. K. Harahap, "Feature Extraction Using Histogram of Oriented Gradient and Hu Invariant Moment for Face Recognition," in *2018 Third International Conference on Informatics and Computing (ICIC)*, 2018, pp. 1-5: IEEE.
- [9] D. Zabala-Blanco, M. Mora, R. J. Barrientos, R. Hernández-García, and J. Naranjo-Torres, "Fingerprint Classification through Standard and Weighted Extreme Learning Machines," *Applied Sciences*, vol. 10, no. 12, p. 4125, 2020.
- [10] C. Wu, J. Zhou, Z.-q. Bian, and G. Rong, "Robust crease detection in fingerprint images," in *2003 IEEE Computer Society Conference on Computer Vision and Pattern Recognition*, 2003. *Proceedings.*, 2003, vol. 2, pp. II-505: IEEE.
- [11] J. Zhou, F. Chen, N. Wu, and C. Wu, "Crease detection from fingerprint images and its applications in elderly people," *Pattern Recognition*, vol. 42, no. 5, pp. 896-906, 2009.
- [12] M. Sarfraz, "Introductory Chapter: On Fingerprint Recognition," in *Biometric Systems: IntechOpen*, 2021
- [13] J. M. Singh, A. Madhun, G. Li, and R. Ramachandra, "A survey on unknown presentation attack detection for fingerprint," *arXiv preprint arXiv:2005.08337*, 2020.
- [14] C. Gottschlich, P. Mihailescu, and A. Munk, "Robust orientation field estimation and extrapolation using semilocal line sensors," *IEEE Transactions on Information Forensics and Security*, vol. 4, no. 4, pp. 802-811, 2009.
- [15] N. Chauhan, M. Soni, V. Anand, and V. Kanhangad, "Fingerprint classification using crease features," in *2016 IEEE Students' Technology Symposium (TechSym)*, 2016, pp. 56-60: IEEE.
- [16] F. Chen, J. Zhou, and C. Yang, "Reconstructing orientation field from fingerprint minutiae to improve minutiae-matching accuracy," *IEEE Transactions on image processing*, vol. 18, no. 7, pp. 1665-1670, 2009.
- [17] [17] W. Bian, Y. Luo, D. Xu, and Q. Yu, "Fingerprint ridge orientation field reconstruction using the best quadratic approximation by orthogonal polynomials in two discrete variables," *Pattern recognition*, vol. 47, no. 10, pp. 3304-3313, 2014.
- [18] Y. Wang, J. Hu, and F. Han, "Enhanced gradient-based algorithm for the estimation of fingerprint orientation fields," *Applied Mathematics and Computation*, vol. 185, no. 2, pp. 823-833, 2007.
- [19] C. Gottschlich, E. Marasco, A. Y. Yang, and B. Cukic, "Fingerprint liveness detection based on histograms of invariant gradients," in *IEEE international joint conference on biometrics*, 2014, pp. 1-7: IEEE.
- [20] L. Wieclaw, "Gradient based fingerprint orientation field estimation," *Journal of Medical Informatics & Technologies*, vol. 22, 2013.
- [21] D. Chen, X. Ji, F. Fan, J. Zhang, L. Guo, and W. Meng, "Comparative analysis of fingerprint orientation field algorithms," in *2009 Fifth International Conference on Image and Graphics*, 2009, pp. 796-801: IEEE.
- [22] S. Jirachaweng, Z. Hou, J. Li, W.-Y. Yau, and V. Areekul, "Residual Analysis for Fingerprint Orientation Modeling," in *2010 20th International Conference on Pattern Recognition*, 2010, pp. 1196-1199: IEEE.
- [23] D. T. Meva, C. Kumbharana, and A. D. Kothari, "The study of adoption of neural network approach in fingerprint recognition," *International Journal of Computer Applications*, vol. 40, no. 11, pp. 8-11, 2012.
- [24] H. Fan, P. Su, J. Huang, P. Liu, and H. Lu, "Multi-band MR fingerprinting (MRF) ASL imaging using artificial-neural-network trained with high-fidelity experimental data," *Magnetic resonance in medicine*, 2021.

- [25] E. Jarocka, J. A. Pruszynski, and R. S. Johansson, "Human touch receptors are sensitive to spatial details on the scale of single fingerprint ridges," *Journal of Neuroscience*, vol. 41, no. 16, pp. 3622-3634, 2021.
- [26] J. Priesnitz, C. Rathgeb, N. Buchmann, C. Busch, and M. Margraf, "An overview of touchless 2D fingerprint recognition," *EURASIP Journal on Image and Video Processing*, vol. 2021, no. 1, pp. 1-28, 2021.
- [27] R. Gupta, M. Khari, D. Gupta, and R. G. Crespo, "Fingerprint image enhancement and reconstruction using the orientation and phase reconstruction," *Information Sciences*, vol. 530, pp. 201-218, 2020.
- [28] N. Brancati, M. Frucci, and G. S. d. Baja, "Reconnecting broken ridges in fingerprint images," in *International Conference on Image Analysis and Processing*, 2009, pp. 739-747: Springer.
- [30] T.-N. Do, "Training neural networks on top of support vector machine models for classifying fingerprint images," *SN Computer Science*, vol. 2, no. 5, pp. 1-12, 2021.
- [31] F. Alonso-Fernandez, J. Fierrez-Aguilar, and J. Ortega-Garcia, "A review of schemes for fingerprint image quality computation," *arXiv preprint arXiv:2207.05449*, 2022.
- [32] A. F. Y. Althabhawe and B. K. O. C. Alwawi, "Fingerprint recognition based on collected images using deep learning technology," *IAES International Journal of Artificial Intelligence*, vol. 11, no. 1, p. 81, 2022.
- [33] A.-M. Dincă Lăzărescu, S. Moldovanu, and L. Moraru, "A Fingerprint Matching Algorithm Using the Combination of Edge Features and Convolution Neural Networks," *Inventions*, vol. 7, no. 2, p. 39, 2022.